University of Pennsylvania
Center for Sensor Technologies

SUNFEST

NSF REU Program
Summer 2004

MINIMIZATION OF DISTORTION AND INCREASING RESOLUTION IN WIDE-ANGLE VIEWING BY MEANS OF ACTUATED MICRO-MIRRORS

NSF Summer Undergraduate Fellowship in Sensor Technologies
William Rivera (Electrical Engineering) – University of Puerto Rico, Mayagüez
Advisor: Dr. Suresh G. K. Ananthasuresh and Dr. Andrew Hicks

ABSTRACT

Mirrors of numerous shapes, including spherical and paraboloidal mirrors, have been employed for many different commercial and industrial uses, despite their tendency to distort and warp images. When the object in consideration is planar and oriented normal to the optical axis of the mirror, the amount of distortion introduced by a paraboloidal mirror is less than the distortion introduced by a spherical mirror. Previous research has found an optimal mirror shape that minimizes distortion of images of planar objects normal to their optical axes.

The goal of this project was to design and construct a single-axis micro-mirror, to form the basis for future work. The micro-mirror construction used a (110) silicon wafer. The design consists of a square mirror supported by two torsional beams. Several design variations were considered to see how these variations affected the fabrication. Due to time limitations, the construction was not completed. It was achieved through the photoresist stripping of the bottom pattern step. Although, the construction was not completed, microfabrication techniques were learned such as mask drawings design, resist processing, photolithography, and the proper use of the Microfab Lab facility equipment. A mechanical modeling of the movement of the single axis micro-mirror was developed. Piezoelectric actuation was explored but due to malfunction of the piezoelectric materials available, it was not possible. Characterization of the voltage differences across the piezoelectric materials was performed to determine why actuation was not possible.

Table of Contents

1. INTRODUCTION

Extensive research into wide-angle viewing (WAV) in recent years has resulted in the use of WAV in military, visual sensors, and automotive applications. The development of vision systems technologies using WAV has made its fusion with other fields such as electronics and micromachining attractive to many researchers. As a result, devices called micro-mirrors (MM) have been developed. MM are microelectromechanical systems (MEMS) that are capable of rotating in order to redirect reflected light. MM has found applications in optical switching, digital light processing (DLP), and optical scanning [1].

Mathematical algorithms and fabrication processes exist for the design of different mirrors shapes to achieve WAV. These algorithms lead to mirrors with paraboloidal and spherical shapes. Unfortunately as long as the mirrors are deformed, distortion is introduced to the images they reflect. Minimization of this image distortion has been achieved by finding an optimal shape between paraboloidal and spherical mirrors [2]. One problem with this kind of mirror is that they are designed for a specific optical axis perpendicular to the tip of the mirror, as shown in Figure 1.

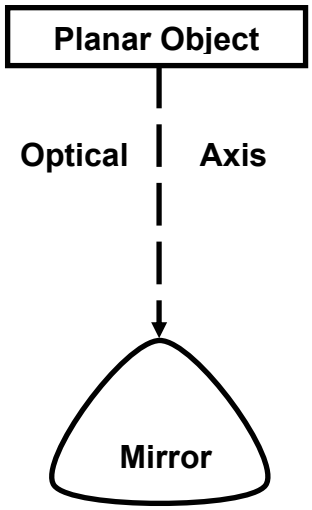

Figure 1: Optical axis of a mirror designed to minimize the distortion in the reflected images.

A long-term objective of this research is to simulate this optimal mirror shape with actuated MM to avoid having to design for just one optical axis. At the same time, the MM increases the resolution of the images since the number of mirrors used to reflect the images is increased.

Presently, this research has three main goals: 1) minimize the distortion in wide angle viewing, 2) study the ways in which the increasing the number of actuated MM can increase the resolution of images, and 3) design and fabricate a device that uses actuated MM to achieve the first two research goals. The tasks assigned for the summer project

were: masks design, microfabrication of the MM, study a mechanical modeling for a single-axis MM and, if time permitted, investigate ways of actuating a macro scale prototype of the MM. The result of the work done through the SUNFEST project made a contribution that forms the basis for future work on the third goal of this research.

2. BACKGROUND

2.1 Wide-angle Viewing (WAV) Distortion

A mirror is a surface capable of reflecting the light that hits it and forms an image on it. Although most commonly used mirrors are planar, some are fabricated in a variety of shapes and sizes such as spherical and paraboloidal. Cameras use mirrors to redirect the images reflected into a set of lenses. Because the field of view of conventional cameras is limited, omnidirectional or WAV cameras have gained popularity for panoramic viewing. The applications for WAV cameras include space optics, robotics, and surveillance. WAV images are achieved by using mounting shown in Figure 2(a).

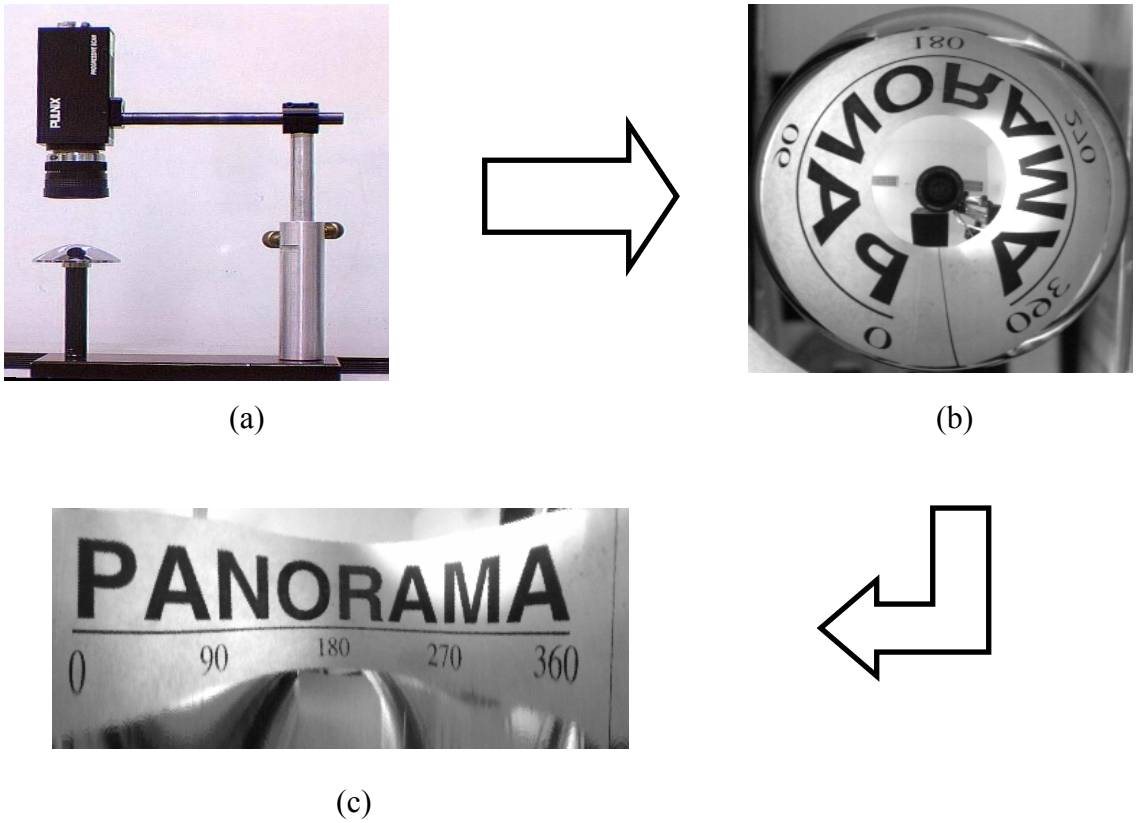

(a) (b)

(c)

Figure 2: (a) WAV setup mounting, (b) warped image, (c) fixed image using computer techniques.

The image obtained from these mirrors is similar to that shown in Figure 2(b). With the help of computer algorithms, this image can be rearranged to better represent reality, as

shown in Figure 2(c). However, even with the use of such special mirrors, the edges of the resulting image are distorted. The amount of distortion depends on the camera's position. The best results are obtained by focusing the mirror through just one optical axis perpendicular to its tip. In this position, image distortion is minimized.

Mathematical algorithms have been developed to find a mirror design that minimizes image distortion in WAV [2]. Although this is a remarkable achievement, to have a WAV image from another point of view, the mirror has to be repositioned. Otherwise, the resulting image will have more distortion.

The use of MM to solve this problem has been suggested. Mathematically, the problem can be represented by a differential equation. If non-planar objects and inclined optical axes are considered, the resulting differential equations cease to have continuous surfaces as solutions. As a future work, the objective of this research is to design and fabricate a versatile device capable of simulating numerous mirror shapes that can emulate the discontinuous solutions. In this manner, if the optical axis is changed, the MM could change their orientation and shape to achieve a position normal to the new optical axis. A description of the proposed method that uses MM is shown in Figure 3.

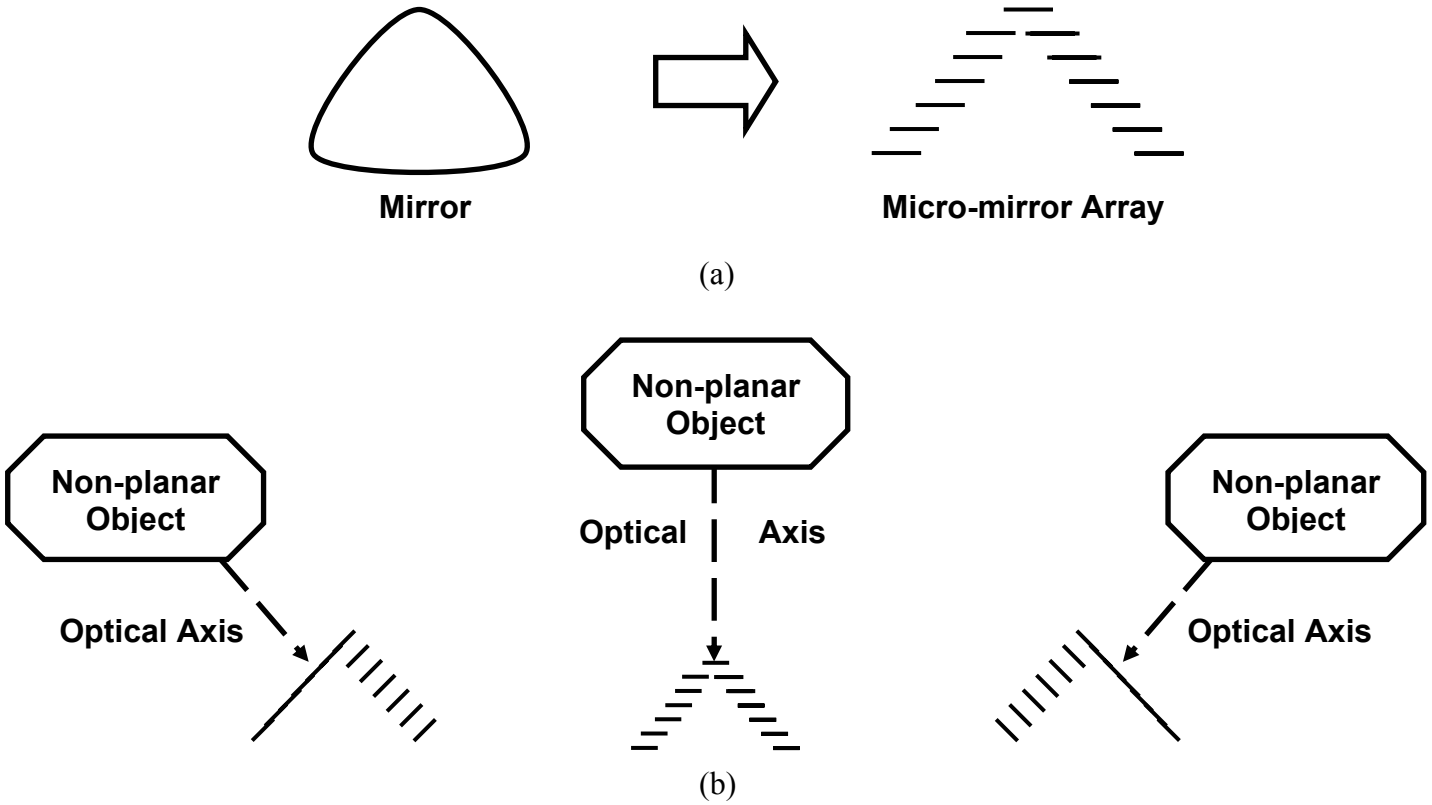

Figure 3: WAV proposed method. (a) Mirror surface simulation through a MM array, (b) MM array orientation change with different optical axis.

2.2 Image Resolution

Pixels are the basic component of computer graphics images. The word comes from the phrase “picture element”. They are the tool by which image colors are programmable in a language that computer understands. The number of pixels per inch (ppi) defines the resolution of an image. Resolution contributes to important characteristics of images such as sharpness, quality, and size. Increasing the resolution of images has effects in applications including space observation, image printing, monitor visualization, remote sensing, and medical studies.

The method by which this research intends to increase images resolution can be understood by following example. Suppose that two pictures are taken from an object at different angles so that they share some part of the picture. Computer techniques can take these two pictures and overlap them only in the shared area. In this way the number of pixels in the shared area increases to the sum of the pixels in that area in the individual pictures. This case is demonstrated by Figure 4.

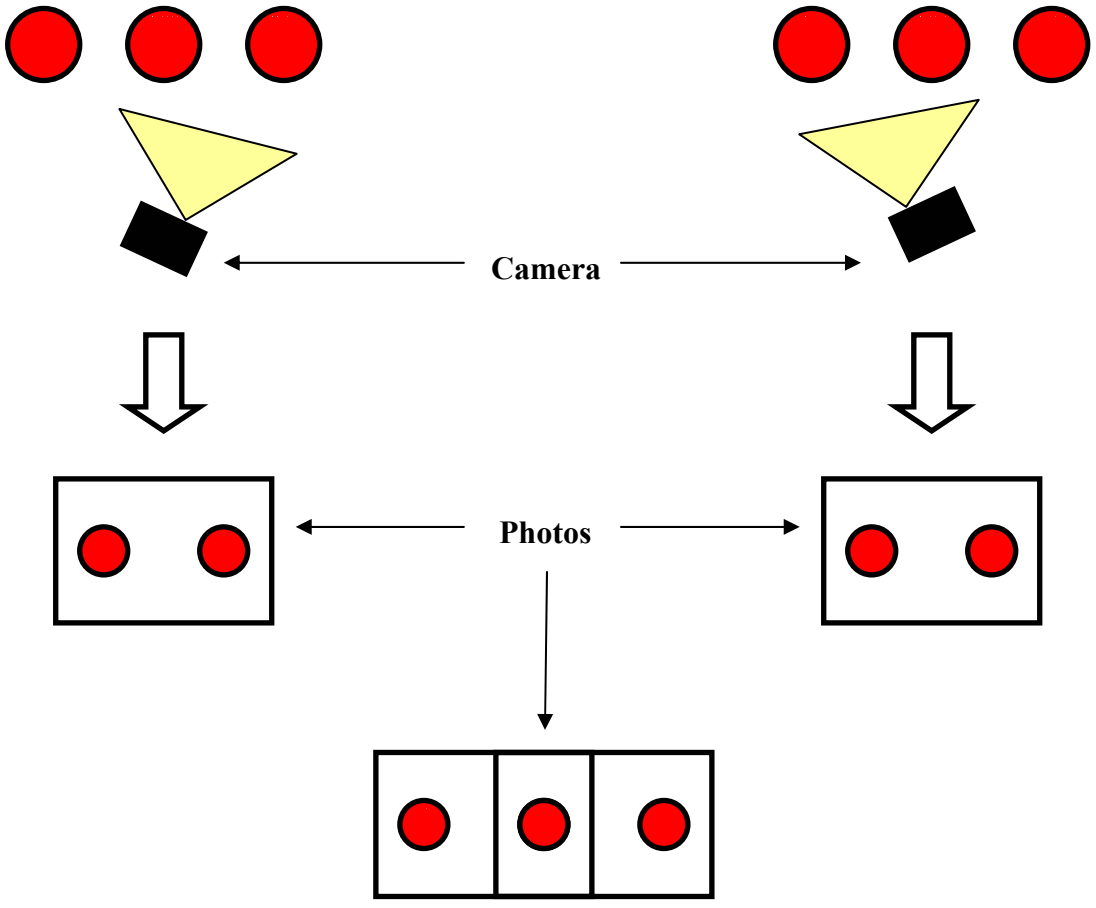

Figure 4: Increase in resolution in overlapped section of pictures taken at different angles. The color is darker in the shared area, indicating that the resolution of that area increased.

Now, instead of having a camera taking single pictures, if a video camera is used, the number of pictures taken could be increased from one picture at a time to 30 pictures per second. If these pictures are overlapped on their shared areas, resolution can be increased. We can go even further if instead of having one single main mirror to receive that light in traditional video cameras, an array of MM is placed. WAV video cameras can use MM not only to reduce the distortion of the fixed images, but to increase the resolution of every single picture captured.

2.3 Fabrication using (110) Silicon Wafers

Silicon single crystal provides uniform, reproducible device characteristics and thus the ability to integrate millions of identical components side by side on a chip. Also, silicon provides a controllable, stable, and reproducible surface layer (SiO_2) which has enabled modern integrated circuit (IC) technology [3]. Crystalline materials such as silicon wafers have a uniform, periodic molecular arrangement through the whole material. Therefore, crystalline materials have specific orientations, which mean that the atoms are arranged in a specific order to form the bonds of the molecules. This orientation defines the properties of the material such as the electrical and the etch rate properties. Also, some applications such as micro heat exchangers choose a specific crystalline orientation of silicon [4]. Figure 5 shows the three basic unit cells or lattices for crystalline materials.

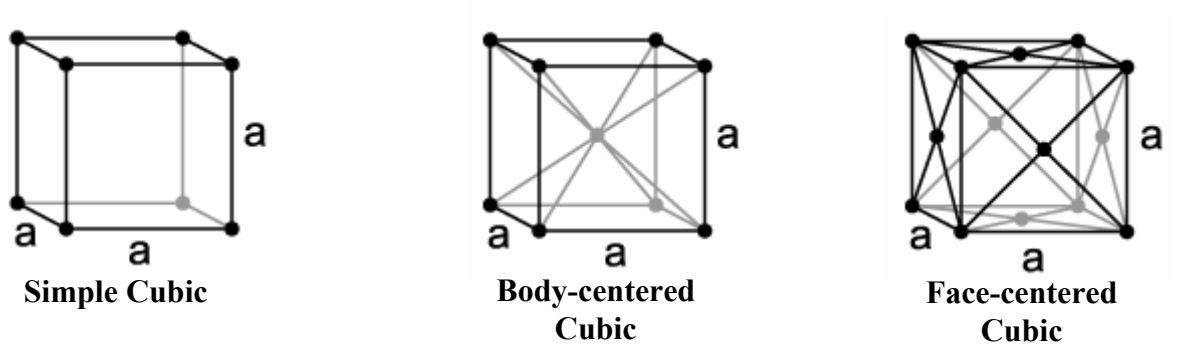

Figure 5: Basic unit cells for crystalline structure materials.

The directions between the atoms in a crystalline material are described by vectors using Cartesian coordinates in this manner: [*xyz*]. In the same way, planes within the crystals are described by what are called Miller indices, which are reciprocals of the planes' interceptions with the Cartesian coordinates' axes. The Miller indices of the planes are written between parentheses. To help visualize these concepts, it is important to note that in cubic lattices the direction of the atoms is perpendicular to the planes that describe them. Figure 6 shows three examples of planes' orientations for crystalline structures.

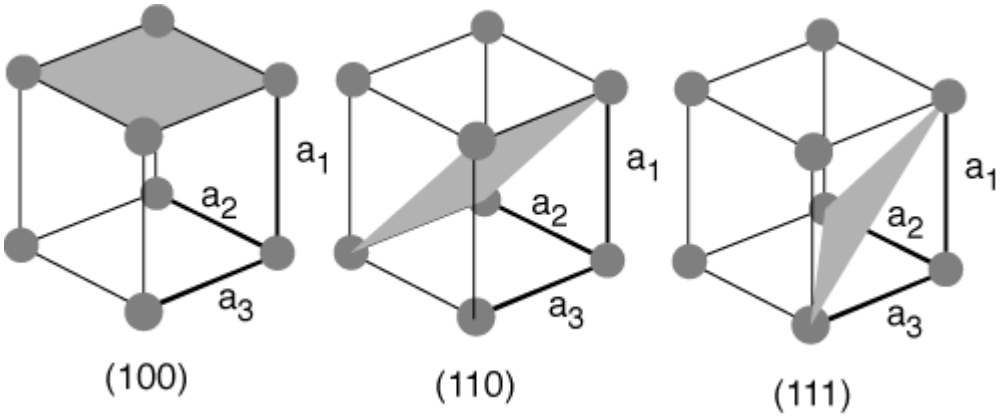

Figure 6: Plane orientation for crystalline materials.

In integrated circuits there are two main silicon crystal orientations: (111) and (100) [5]. For the fabrication of the MM, silicon wafers that have (110) plane orientations were chosen. This orientation permits fabrication of structures with narrow trenches with vertical side walls. Characteristic desired for the mirrors' fabrication since it requires etching the wafer as straight as possible to have a high aspect ratio. Also, the fabrication requires fine structures as straight beams and serpentine spring beams.

3. FABRICATION OF THE DESIGN

3.1 Process Flow

In order to fabricate the MM, a process flow, of the steps to construct it was designed. It is shown in Figure 7. The process flow offered a method to study and understand all the processes involved in the MM fabrication. The process flow starts with the selection of the orientation of the silicon wafer. Then, the wafer is put into an oxidation furnace until a SiO_2 layer of desired thickness is grown. This layer, after patterning, serves as a mask for KOH etching. Next, a layer of positive photoresist is spun onto its surfaces, and it is soft-baked to harden the photoresist. The wafer is then placed on the photolithography machine and is aligned with the top mask in order to expose the wafer to ultra violet (UV) light for 14 seconds. The UV light changes the chemical composition of the exposed portion of the photoresist be exposed, making it more soluble. In this manner, the pattern of the bottom mask is transferred to the bottom wafer surface. After that, the wafer is introduced into a solvent to remove the exposed photoresist. Other solvents are used to take out the uncovered SiO_2 and the unexposed photoresist. These steps serve as a preparation for KOH etching which removes the pure silicon where there is no SiO_2. KOH etching is performed on the bottom surface first because the top surface, which is the reflective part of the MM, will form a thin plate. The etch-rate varies for the different crystal orientation structures. For that reason, when KOH etching, one has to be aware of the time that the wafer is been etched. Also, it is possible to estimate the desired amount of etching by visual inspection.

After the wafer is etched on the bottom surface a layer of photoresist is spun on both sides to prepare the wafer to be exposed to UV light on the top surface. Then, the wafer and the bottom masks are aligned in the photolithography machine, and the pattern of the top masks is transferred to the top surface of the silicon wafer. Then the stripping processes are repeated. At the end only a pure silicon structure is left.

Figure 7: Process Flow of the MM fabrication

Step 1: Selection of the silicon wafer

Step 2: Silicon layer oxide growth

Step 3: Photoresis1t Layer Spinning

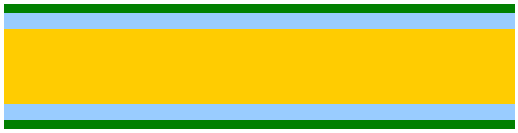

Step 4: Soft Baking

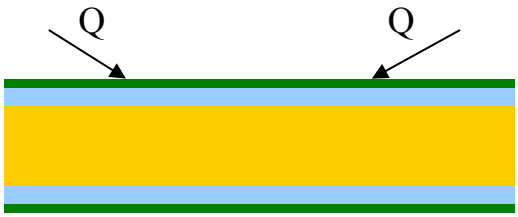

Step 5: UV Exposure of the single axis MM on the bottom mask

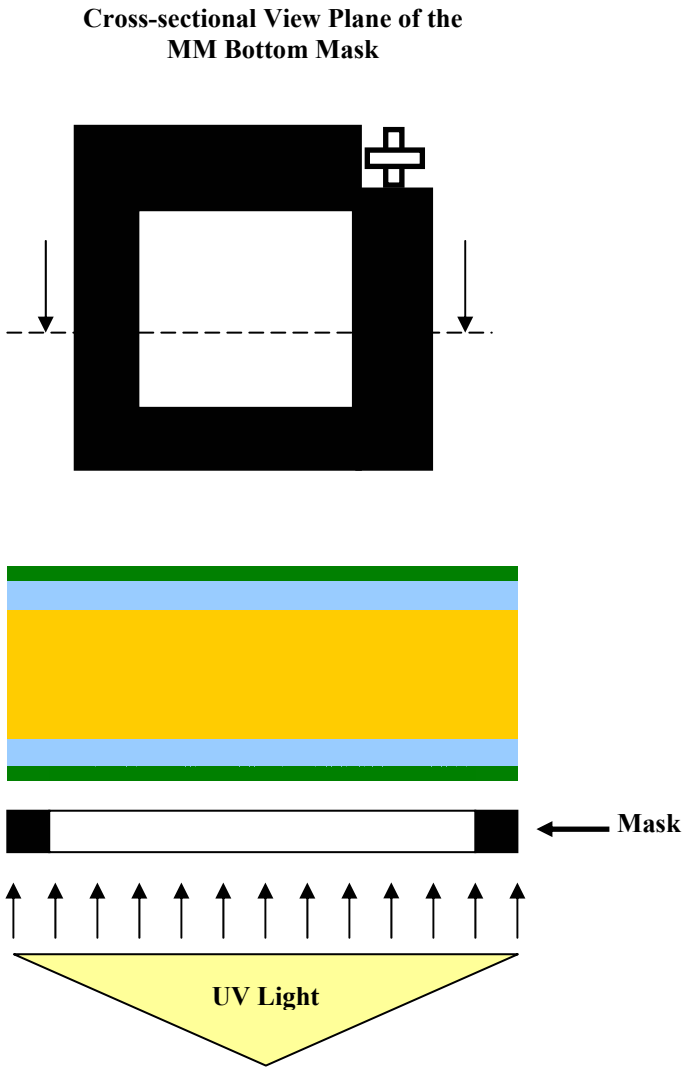

Silicon wafer with (110) orientation

Thin layer of silicon oxide

Resist Layer

Exposed Resist Layer

Q = Heat

Step 6: Development of the photoresist

Step 7: Oxide Etching

Step 8: Photoresist Stripping

Step 9: Bottom KOH etching

Step 10: Photoresist Layer Spinning

Step 11: Soft Baking

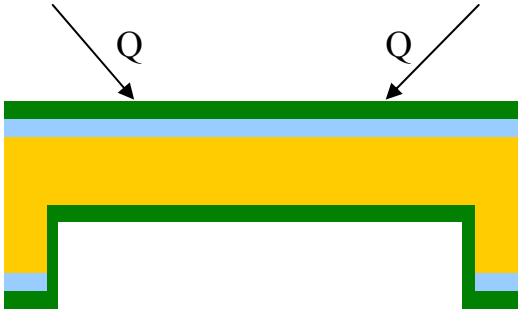


Silicon wafer with (110) orientation


Thin layer of silicon oxide


Resist Layer

Q = Heat

Step 12: UV Exposure of the single axis MM on the top mask

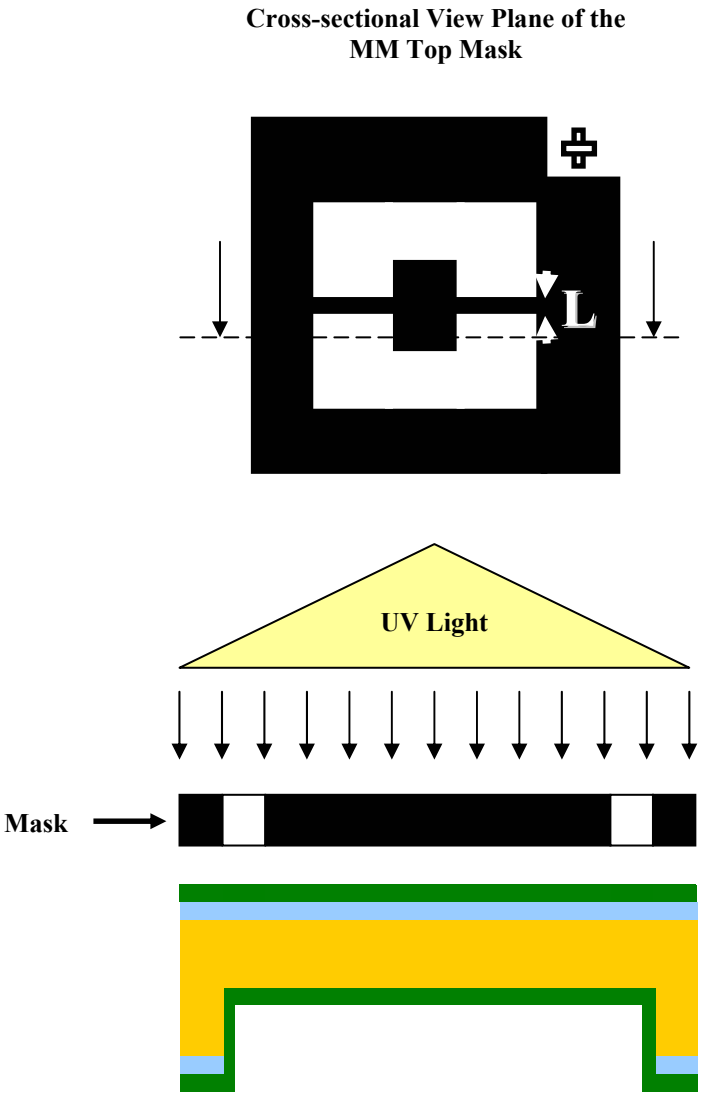

Step 13: Development of the photoresist

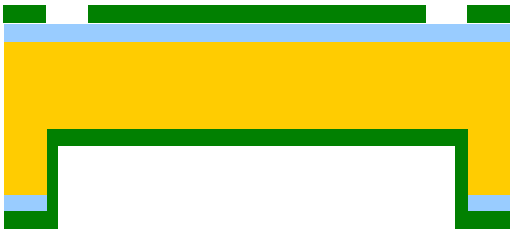

Step 14: Oxide Stripping

Step 15: Photoresist Stripping

Step 16: Top KOH Etching

Step 17: Oxide Stripping

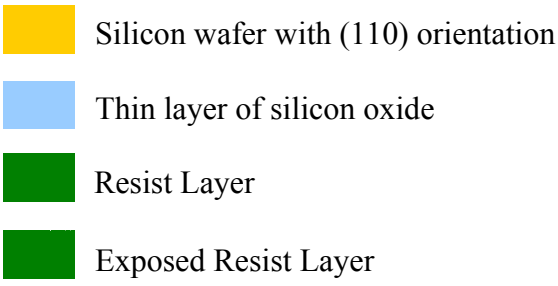

3.2 AutoCAD Design

The MM designs were done using AutoCAD. The designs contain the shapes for two different masks: the top and the bottom masks. The top mask was used to expose the silicon wafer on the polished side and the bottom mask on the opaque side. The drawings include the designs for two kinds of MM. The first is a single-axis MM, consisting of a square plate supported by two torsional beams as shown in Figure 8(a). The beams thickness was varied to investigate how thin they could be made. They had thickness of 25μm, and 50μm, and 75μm. The second kind of MM has serpentine spring beams; it is shown in Figure 8(b). This variation in the design was to explore other fabrication possibilities.

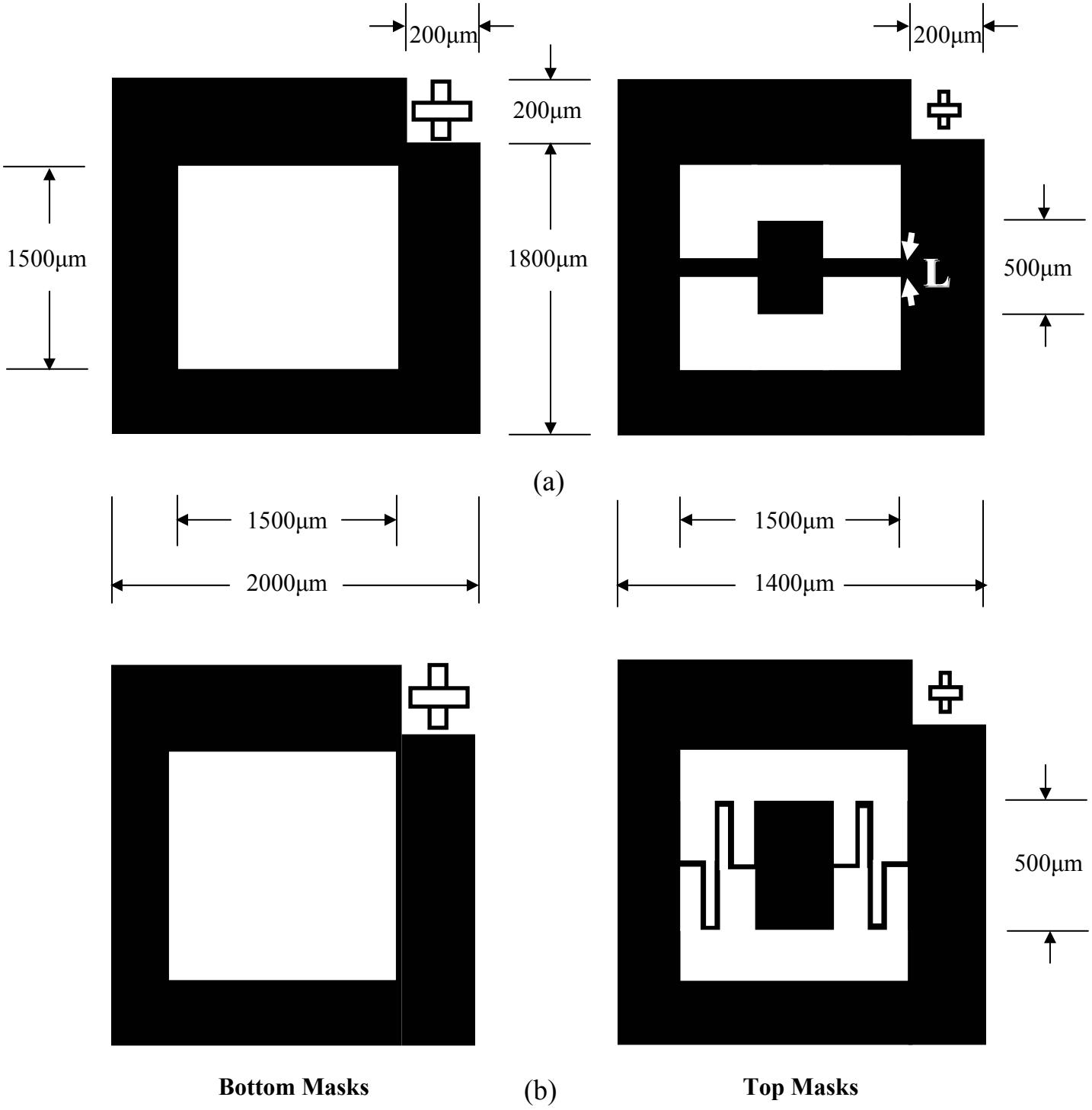

Figure 8: Drawings of the MM designs. (a) Single-axis MM, (b) Serpentine spring MM

4. RESULTS

4.1 Fabrication Results

The masks design was completed using AutoCAD and fabricated in the Microfab Lab facility. The mask is shown in Figure 9.

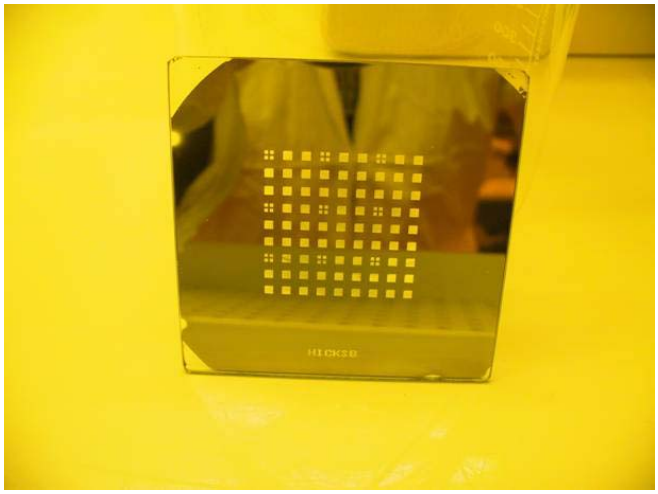

Figure 9: Bottom mask with corrected polarity.

The other fabrication result was the construction of the MM. Due to time limitations, the construction of MM was stopped after Step 8 in the process flow was finished. The unfinished silicon wafer is shown in Figure 10.

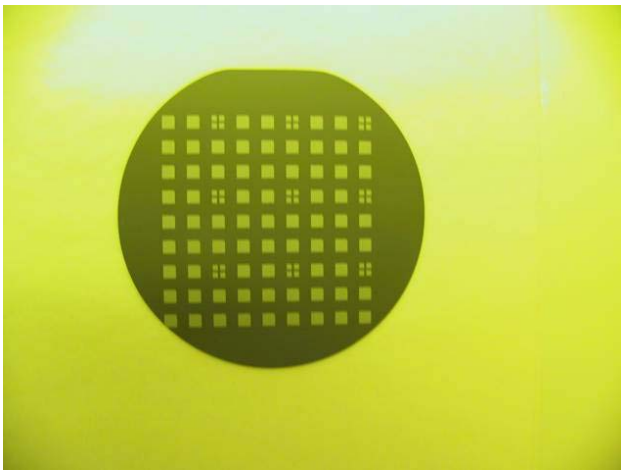

Figure 10: Silicon wafer used for the MM fabrication. This is how it looks after the Step 8 of the process flow was finished.

4.2 Mechanical Modeling

The mechanical modeling task was accomplished through the use of a macro scale prototype of a single-axis mirror. The material used for the prototype was polycarbonate and the Excimer Laser machine was used to cut it. The model considers the dependence of the force and torque on the prototype dimensions. Also, torsional properties of the material were considered with a maximum rotational movement of 10°. For polycarbonate two values of Young's modulus *E* and Poisson's ratio *v* were considered. Figure 11 shows a drawing of the prototype along with the forces/moments and dimensions.

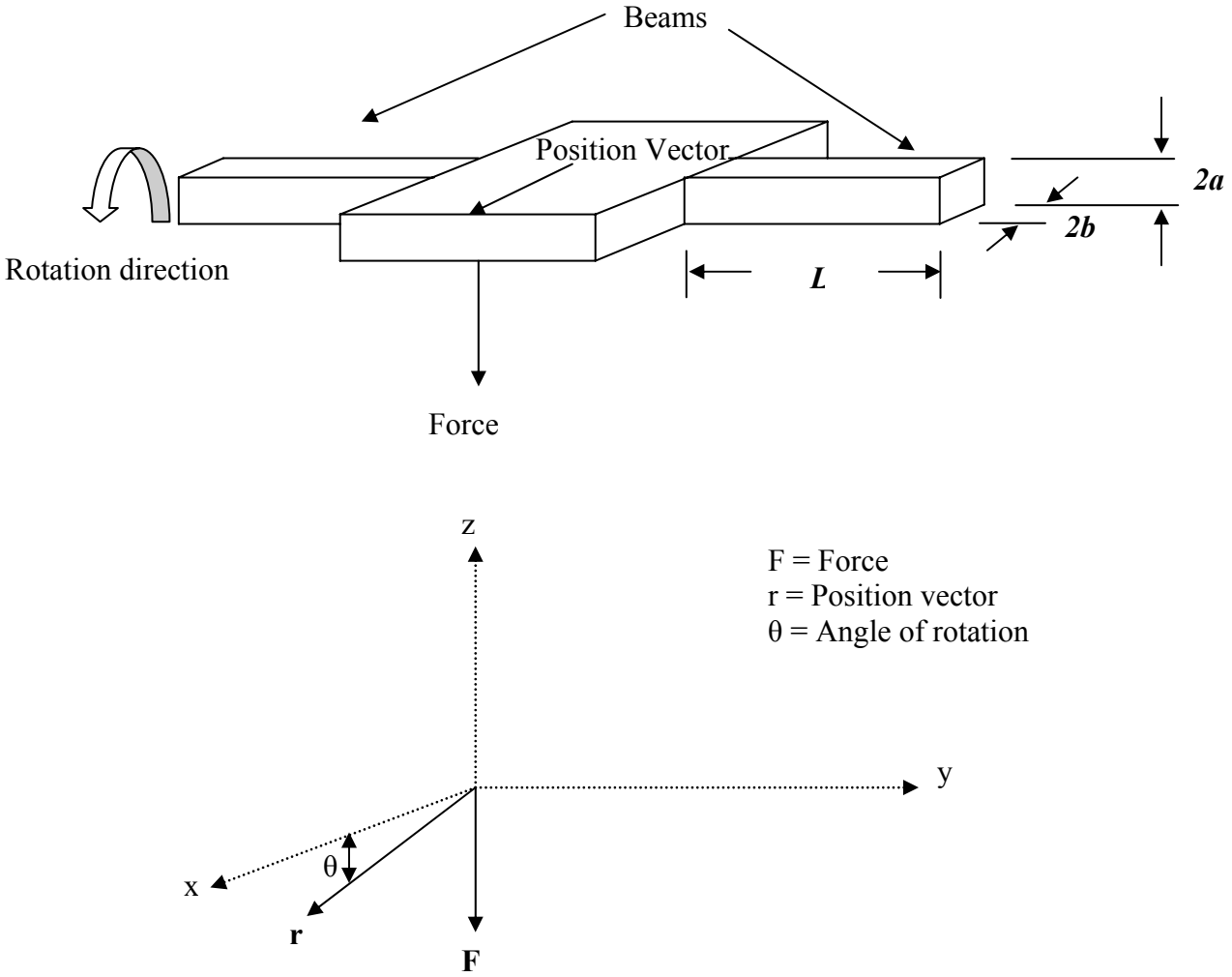

Figure 11: MM prototype drawing and its force diagram representation.

Geometrical properties of the solid rectangle beams:

$$Width = \boldsymbol{2a} \rightarrow \boldsymbol{a} = \frac{Width}{2} = 0.01\text{in}$$

$$Thickness = \boldsymbol{2b} \rightarrow \boldsymbol{b} = \frac{Thickness}{2} = 0.0625\text{in}$$

$\boldsymbol{L} = 0.369\text{in}$

Modulus of rigidity:

$$G = \frac{E}{2(1+v)} \Rightarrow v \approx 0.4 - 0.5 \; and \; E = 2.9,6.9GPa \;\; for \;\; polycarbonate$$

Function of cross-sectional geometry:

$$K = ab^3\left[\frac{16}{3} - 3.36\frac{b}{a}\left(1 - \frac{b^4}{12a^4}\right)\right] = 0.003288\,mm^4$$

Toque calculation:

$$\mathbf{T} = \mathbf{r} \text{ x } \mathbf{F} = \begin{vmatrix} a_x & a_y & a_z \\ r_x & 0 & -r_z \\ 0 & 0 & -F \end{vmatrix}$$

$\mathbf{T} = r_x F \, \mathbf{a_y} = Fr \cos(\theta) =$

$$T = Torque = \frac{\theta GK}{l}$$

$$F = \frac{T}{r\cos(\theta)}$$

Solving for the torque and force for a maximum angle θ =10° gives:

At E = 2.4 GPa and v = 0.4
T = 0.1627 N·m, F = 32.5173 N

At E = 6.9 GPa and v = 0.4
T = 0.4677 N·m, F = 93.4871 N

At E = 2.4 GPa and v = 0.5
T = 0.1518 N·m, F = 30.3494 N

At E = 6.9 GPa and v = 0.5
T = 0.4365 N·m, F = 87.2547 N

4.3 Prototype Actuation

The actuation of the macro scale polycarbonate prototype was attempted. The intention was to implement a method that could be reproduced in the micro scale. The proposed method was to make a piezoelectric material to move the MM replica of polycarbonate. The piezoelectric material plate shown in Figure 12 has length = 1.25", width = 0.125" and thickness = 0.015". (The dime is included to show the scale of the object.)

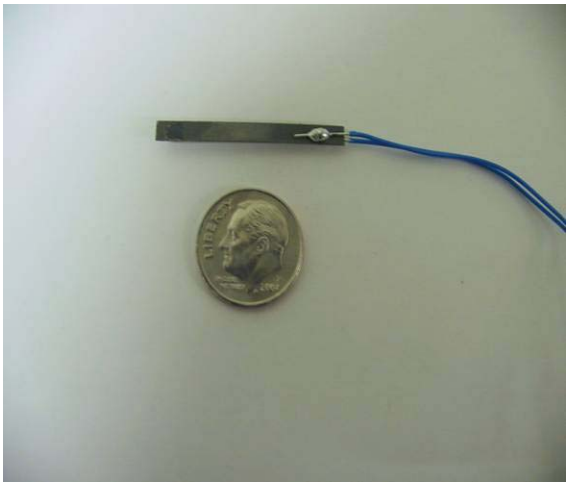

Figure 12: Piezoelectric material used for the actuation try.

To see appreciable movement, it was necessary to apply 120V across the thickness of the piezoelectric material. The movement was measured and compared to the results of the mechanical model. The voltage across the thickness of the piezoelectric material was measured along the length of each piece. The measurements are shown in Figure 13.

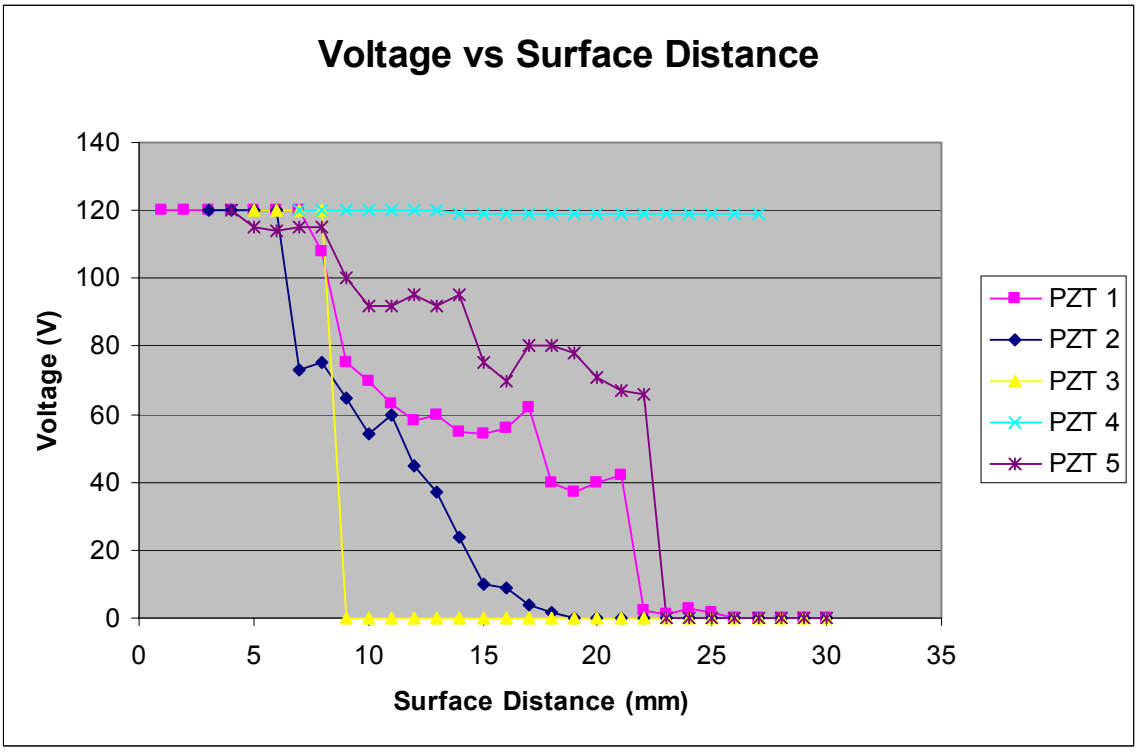

Figure 13: Voltage distribution along the length of the piezoelectric materials.

5. DISCUSSION AND CONCLUSIONS

During the summer, some complications slowed down the completion of the assigned tasks. First, the translator of Microfab Lab was not able to read the AutoCAD file that contained the mask drawings. Much time and effort was spent correcting the file to make it readable. Another factor was that the first fabricated masks had the wrong polarity, so what was supposed to be a dark section that wouldn't allow UV light to pass was clear. In the same way, what was supposed to be the clear section was dark. The masks with the wrong polarity are shown in Figure 14.

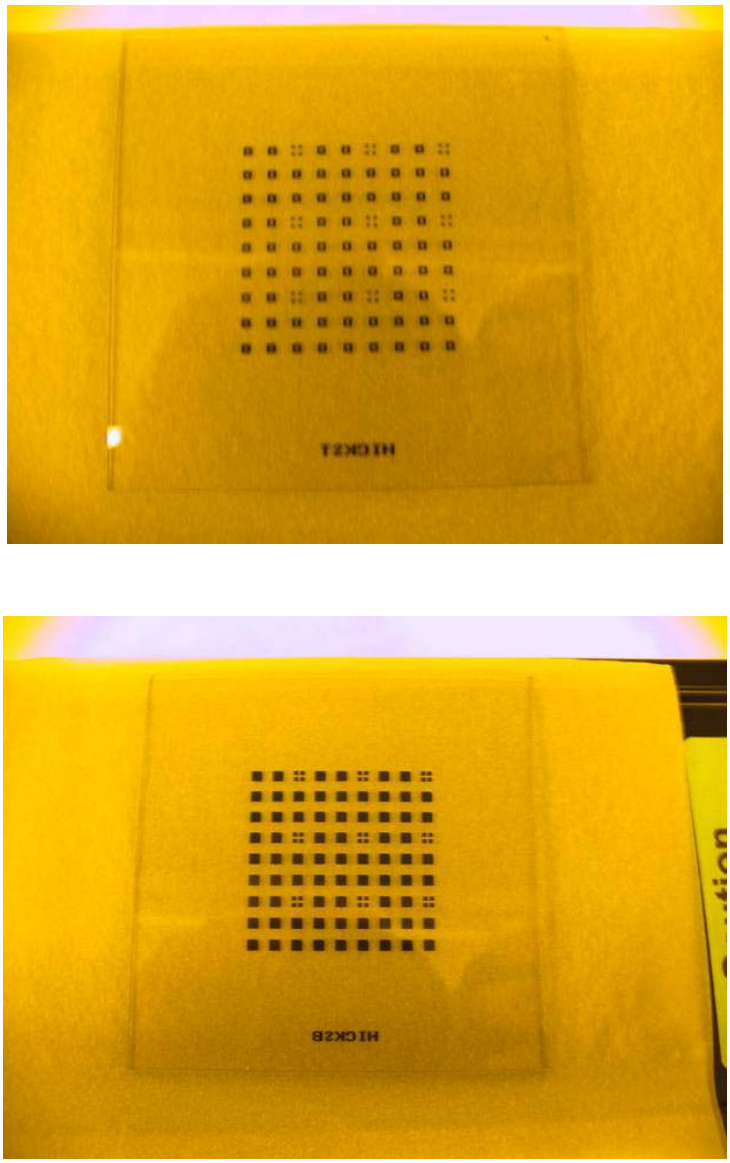

Figure 14: Fabricated masks with wrong polarity.

Although the completion of the fabrication of the MM was not possible, the wafer processing could be continued along the lines indicated in this report.

Of the five pieces of piezoelectric materials that were available, only two showed movement. However, of these two, only one moved well. In Figure 13 the results for the two piezoelectric materials that moved are denoted as PZ1 and PZ5. The measurements from the plate that move very well (PZ1) show that the voltage across the material is almost constant, which means that the charge distribution across its length is almost constant, too. In the case of plate PZ5, it does not have a uniform charge distribution

across it. This suggests that there should be a minimum voltage and distance to make this kind of material move.

6. RECOMMENDATIONS

To continue this work in the future, finish the fabrication of the single-axis MM, and explore two-axis MM fabrication. I recommend finishing the fabrication and trying to design and implement the actuation at the macro and micro levels. Since the wafers are thinner than the ones currently used in the Microfab Lab, it is important when KOH etching to check how deeply the wafer is etched at frequent intervals. Also, for the actuation, it will be important to make the proper selection of the piezoelectric materials used. Another alternative for the actuation is to use a compliant mechanism to amplify the movement of the piezoelectric materials.

7. ACKNOWLEDGMENTS

I would like to thank the National Science Foundation for the support for undergraduate students and give the opportunity to experience research. Also, I would like to express my gratitude to the SUNFEST program for giving me the opportunity to be a participant. The more special thanks are for my advisors Dr. Ananthasuresh and Dr. Hicks for their tremendous advising and availability, and for giving me the opportunity to work with them. Finally, I would like to thank Prof. Van der Spiegel, Prof. Santiago, Prof. Lee, Prof. Bloomfield, Prof. Zemel, Salvador, and Dr. Scott Slavin for their support and help during this research.

8. REFERENCES

1) http://www.i-o.com/content/includes/MEMSmirror.pdf
H. Goldberg, D. Yu, B. Reichert, K. Speller, *A MEMS Mirror for Optical Scanning*, Applied MEMS, Inc.

2) R. A. Hicks, R. Bajcsy, *Catadioptric Sensors that ApproximateWide-angle Perspective Projection*, CVPR 2000. pp. 545-551.

3) J. D. Plummer, M. D. Deal, P. B. Griffin, *Silicon VLSI Technology: Fundamentals, Practice and Modeling*, Prentice Hall, New Jersey, 2000, pp 7-8, 94-96,201-281

4) S. Kang, Y. Chen, G. Chang, *The Manufacture and Test of (110) Orientated Silicon Based Micro Heat Exchanger*, Tamkang Journal of Science and Engineering, Vol. 5, 2002, pp. 129-136

5) M. Madou, *Fundamentals of Microfabrication*, CRC Press, New York, 1997, pp. 1-86.

6) K. J. Gabriel, *Engineering Microscopic Machines*, Scientific American, September 1995, pp. 150-153

7) D. J. Bishop, C. R. Giles, S. R. Das, *The rise of Optical Switching*, American, January 2001, pp. 88-94

8) G. T. A. Kovacs, *Micromachined Transducers Sourcebook*, McGraw-Hill, New York, 1998, Ch. 5

9) http://www.ee.byu.edu/cleanroom/./EW_orientation.phtml

10) http://whatis.techtarget.com/definition/0,,sid9_gci212793,00.html

11) http://www.opticsforkids.org/resources/Intro_to_Mirrors_and_Lenses.pdf

12) http://www.bmva.ac.uk/bmvc/1998/pdf/p021.pdf